# Experimental results of Discrete Time Variable Structure Control for Dynamic Positioning of Marine Surface Vessels


**P. Raspa * F. Benetazzo * G. Ippoliti * S. Longhi *
Asgeir J. Sørensen ****

* *Dipartimento di Ingegneria dell'Informazione, Università Politecnica delle Marche, Via brecce Bianche, 60131 Ancona AN, Italy
email: (p.raspa, f.benetazzo, g.ippoliti, sauro.longhi)@univpm.it*
** *Department of Marine Technology, the Norwegian University of Science and Technology (NTNU), NO-7941 Trondheim, Norway
e-mail: asgeir.sorensen@ntnu.no*



**Abstract:** This paper presents a Discrete-Time Variable-Structure Control (DTVSC) for the dynamic positioning system of a marine supply vessel to guarantee robustness with respect to disturbances and parametric variations. The control system is combined with a wave compensation based on a Multirate Extended Kalman Filter (MR-EKF). The dynamic positioning system is provided by a DTVS controller. The proposed solution has been tested on a real vessel and the experimental results are corroborated by simulations.



Keywords: Ship nonlinear model, variable structure control.


## 1. INTRODUCTION

Offshore exploration and exploitation of hydrocarbons have opened up an era of dynamically positioned (DP) vessels. The number of vessels equipped with dynamic positioning (DP) systems rose in the recent years due to increasing oil and gas exploration at sea. The DP is an autonomous control system that acts to maintain the vessel position and the angle of direction at a reference point by means of the vessel propulsion and maneuvering thrusters. Knowledge of thruster allocation, combined with information from the sensors (GPS, gyroscopes, etc), is used to calculate the steering angle and the thrust for each thruster. The control action maintains the desired position and orientation according to a navigation path or a specific task (absolute or relative DP). The dynamic positioning system is decisive in those situations in which the position of the unit is bound to a specific point on the seabed (absolute DP), or it is related to a moving unit, like when the ship is operating with other vessels or for remotely operated underwater vehicles. A dynamically positioned (DP) vessel is by the International Maritime Organization (IMO) and the certifying class societies (DNV, ABS, LR, etc.) defined as a vessel that maintains its position and heading (fixed location or pre-determined track) exclusively by means of active thrusters, Sorensen [2011]. Other solutions like position mooring consider the aid of mooring lines, see Nguyen and Sorensen [2009].

Up to now, most dynamic positioning systems have been used for positioning drill ships in deep water and other offshore operations, such as diving support and anchor handling. Furthermore, DP systems have been applied increasingly to shuttle tankers during offloading operation with a floating production storage and offloading (see Sorensen [2011] and Fossen [2011]). The first DP systems were designed using conventional PID controllers in cascade with low pass and/or notch filters to suppress the wave induced motion components. From 1980, a new model-based control concept, which is based on stochastic optimal control theory and Kalman filtering techniques, was employed to address the DP problem by Balchen et al. [1980]. Later extensions and modifications of the latter work have been proposed by numerous authors, see Sorensen [2011] and simulated therein. In Xia et al. [2005] and in Tannuri and Agostinho [2010] the sliding mode control is used with a Passive Nonlinear Observer for the DP problem.

This paper presents an innovative solution for the DP control system of a vessel which is based on Discrete-Time Variable Structure Controller (DTVSC) and Wave Filtering using a (Multi-rate) Extended Kalman Filter. The introduction of DTVSC allows to directly take into account the issue of control law digitalization . Moreover it ensures robustness with respect to model uncertainties and input disturbances acting on the actuators. An Extended Kalman filter (EKF) is designed in order to estimate the disturbances induced by the first order wave forces on the thruster. This is done to minimize the thruster efforts. The estimation is improved by means of a Multi-Rate Extended Kalman Filter (MREKF) which allows to take into account differences in working frequency of the sensors. The proposed solution has been tested on a real vessel and the experimental results are corroborated by simulations.

The paper is organized as follows. The kinematic and dynamic equations, the thruster allocation and the wave model are presented in Section 2. The filter techniques are

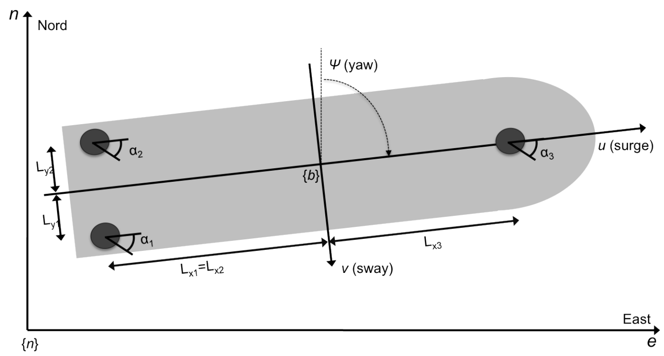


Fig. 1. Vessel Reference frames

discussed in Section 3. The control system, in particular the DTVS controller, is reported in Section 4. Experimental and Simulated results are presented in Section 5. The paper ends with conclusions and comments.

## 2. MATHEMATICAL MODEL OF DP VESSEL

The motion superposition model is the most commonly adopted for ship motion control system design Perez et al. [2004]. Motion can be conceptually decomposed as superposition of three contribution:

- **slowly-varying disturbance motion** produced by second-order waves effects, current and wind;
- **control-induced motion** described by a manouvering model, clarifying the relationship between control action and its effects on the motion (the dynamics is very slow for the class of offshore supply vessels, thus is referred as Low Frequency (LF) dynamics);
- **wave-induced motion** where the wave frequency oscillatory motion induced by first-order waves is described by a seakeeping model, this dynamics is referred as Wave Frequency (WF) dynamics.

### *2.1 Manoueuvering Model*

The motion of a surface vessel for the development of a dynamic positioning system is described by a model which is based on the common assumption that only horizontal forces must be counteracted, as stated in Fossen [2011]. In this hypotheses the generalized velocity vector $\boldsymbol{\nu} \triangleq [u, v, r]^T$ in the ship body-fixed frame $\{b\}$ is considered, where $u$ is the surge velocity, $v$ is the sway velocity and $r$ the yaw rate, see Fig. 1. Ship position is referred to the local geographical inertial North-east-down frame $\{n\}$, fixed to the Earth and described by the generalized position $\boldsymbol{\eta} \triangleq [n, e, \psi]^T$, where $n$ and $e$ are the ship position in the $\{n\}$ frame and $\psi$ is the ship orientation referred to the $n$ frame.

Under the assumption of low-speed manoeuvring the quadratic terms of velocity, Coriolis terms and non-linear damping terms are neglected. With the recalled notation, the DP model is described by the following dynamics:

$$\boldsymbol{M}\dot{\boldsymbol{\nu}}_{LF} + \boldsymbol{D}\boldsymbol{\nu}_{LF} = \boldsymbol{\tau}_c + \boldsymbol{\tau}_{env}, \tag{1}$$

where $\boldsymbol{\nu}_{LF}$ is the low-frequency generalised velocity vector, $\boldsymbol{M}$ is the rigid body generalised mass, which includes inertia and added mass, $\boldsymbol{D}$ is the linear damping component, $\boldsymbol{\tau}_c$ and $\boldsymbol{\tau}_{env}$ are the generalized control force and environmental disturbances, respectively. The kinematic equation has the following form:

$$\dot{\boldsymbol{\eta}}_{LF} = \boldsymbol{R}(\psi)\boldsymbol{\nu}_{LF} = \begin{bmatrix} \cos\psi & -sin\psi & 0 \\ \sin\psi & cos\psi & 0 \\ 0 & 0 & 1 \end{bmatrix} \boldsymbol{\nu}_{LF}, \tag{2}$$

where $\boldsymbol{\nu}_{LF}$ is the low-frequency ship position and the matrix $\boldsymbol{R}(\psi)$ describes rotation from $\{b\}$ frame to $\{n\}$ frame.

### *2.2 Environmental Disturbances*

Environmental disturbances include both slowly varying and high frequency forces. The slowly varying disturbances include second order wave drift, ocean currents and wind forces. These effects are modeled by a bias $b$, described by the following dynamic equation:

$$\dot{\boldsymbol{b}} = \boldsymbol{w}_b, \tag{3}$$

where $\boldsymbol{w}_b \sim \mathcal{N}(0, \boldsymbol{Q}_b)$ is a white noise with zero mean and covariance matrix $\boldsymbol{Q}_b$ Fossen [2011]. This environmental disturbance force, referred to ship body frame $\{b\}$ has the form (Fossen [2011]):

$$\boldsymbol{\tau}_{env} = \boldsymbol{R}(\psi)^T b.$$

First order wave forces effects on ship motion on the 3DOF are modeled in the Wave Frequency (WF) Dynamics by 3 second order systems of which state space form is:

$$\underbrace{\begin{bmatrix} \dot{\xi}_1 \\ \dot{\xi}_2 \\ \dot{\xi}_3 \\ \dot{\xi}_4 \\ \dot{\xi}_5 \\ \dot{\xi}_6 \end{bmatrix}}_{\dot{\boldsymbol{\xi}}} = \underbrace{\begin{bmatrix} 0 & 1 & 0 & 0 & 0 & 0 \\ -\omega_{0_n}^2 & -2\lambda_{w_n}\omega_{0_n} & 0 & 0 & 0 & 0 \\ 0 & 0 & 0 & 1 & 0 & 0 \\ 0 & 0 & -\omega_{0_e}^2 & -2\lambda_{w_e}\omega_{0_e} & 0 & 0 \\ 0 & 0 & 0 & 0 & 0 & 1 \\ 0 & 0 & 0 & 0 & -\omega_{0_\psi}^2 & -2\lambda_{w_\psi}\omega_{0_\psi} \end{bmatrix}}_{\boldsymbol{A}_w}$$

$$\underbrace{\begin{bmatrix} \xi_1 \\ \xi_2 \\ \xi_3 \\ \xi_4 \\ \xi_5 \\ \xi_6 \end{bmatrix}}_{\boldsymbol{\xi}} + \underbrace{\begin{bmatrix} 0 & 0 & 0 \\ K_{w_n} & 0 & 0 \\ 0 & 0 & 0 \\ 0 & K_{w_e} & 0 \\ 0 & 0 & 0 \\ 0 & 0 & K_{w_\psi} \end{bmatrix}}_{\boldsymbol{E}_w} \boldsymbol{w}_w; \quad \boldsymbol{\eta}_{WF} = \underbrace{\begin{bmatrix} 0 & 1 & 0 & 0 & 0 & 0 \\ 0 & 0 & 0 & 1 & 0 & 0 \\ 0 & 0 & 0 & 0 & 0 & 1 \end{bmatrix}}_{\boldsymbol{C}_w} \begin{bmatrix} \xi_1 \\ \xi_2 \\ \xi_3 \\ \xi_4 \\ \xi_5 \\ \xi_6 \end{bmatrix} \tag{4}$$

where the components of $\boldsymbol{\eta}_{WF}$ are three linear ship wave response models in surge, sway and yaw with state vector $\boldsymbol{\xi} \in \Re^6$, the terms $K_{w_i} = 2\lambda_{w_i}\omega_{0_i}\sigma_{w_i}$ with $i \in \{n, e, \psi\}$ represent constant gains, where $\sigma_{w_i}$ are the wave intensities, $\lambda_{w_i}$ are damping coefficients and $\omega_{0_i}$ are the dominating wave frequency for $i \in \{n, e, \psi\}$. These parameters are estimated using the technique described in Fossen and Perez [2009] when there are significant changes in heading and at regular intervals of 20 minutes, which is the time period for which the sea state can be considered to be stationary. Assuming that the vessel is in position control mode the measured motion $\boldsymbol{\eta}_m$ is recorded and detrended to provide an off-line estimation of the wave induced motion $\hat{\boldsymbol{\eta}}_{WF}$. The white noise $\boldsymbol{w}_w = [w_{w_n}, w_{w_e}, w_{w_\psi}]^T \sim \mathcal{N}(0, \boldsymbol{Q}_w)$ has with zero mean and covariance matrix $\boldsymbol{Q}_w$ is estimated from the sample covariance of prediction errors $\boldsymbol{\eta}_\epsilon = \hat{\boldsymbol{\eta}}_{WF} - \boldsymbol{\eta}_{WF}$, Fossen [2011].

### 2.3 Thruster Allocation

Marine vessels with $n$ DOF are characterized by $n$ generalized control forces $\boldsymbol{\tau}_c \in \Re^n$ which are distributed among the $r$ thrusters in terms of control inputs $\boldsymbol{u} \in \Re^r$:

$$\boldsymbol{\tau}_c = \boldsymbol{T}(\boldsymbol{\alpha})\boldsymbol{u} \tag{5}$$

where $\boldsymbol{u}$ is the thrust force vector. The thruster configuration matrix $\boldsymbol{T}(\boldsymbol{\alpha})$ depends on the location and orientation of the thrusters. The considered 3DOF offshore supply vessel has three azimuth thrusters, as shown in Figure 1. Thruster configuration matrix $\boldsymbol{T} = \boldsymbol{T}(\boldsymbol{\alpha})$ follows:

$$\boldsymbol{T}(\boldsymbol{\alpha}) = \begin{bmatrix} c(\alpha_1) & c(\alpha_2) & c(\alpha_3) \\ s(\alpha_1) & s(\alpha_2) & s(\alpha_3) \\ -l_{y1}c(\alpha_1) - l_{x1}s(\alpha_1) & l_{y2}c(\alpha_2) - l_{x2}s(\alpha_2) & l_{x3}s(\alpha_3) \end{bmatrix} \tag{6}$$

Where $c(\alpha_i)$ and $s(\alpha_i)$ stand for $\cos(\alpha_i)$ and $\sin(\alpha_i)$ respectively. Referring to the thruster configuration matrix in (6), Figure 1 shows that the allocation of the 3 azimuthal thrusters is symmetrical with respect to the longitudinal axis of the vessel. The input disturbances $\boldsymbol{d}$ are modelled as slowly varying bias, described by the dynamics equation $\dot{\boldsymbol{d}} = \boldsymbol{w}_d$, where $\boldsymbol{w}_d \sim \mathcal{N}(\boldsymbol{0}, \boldsymbol{Q}_d)$ is a white noise source. Therefore the inclusion of input disturbances transforms the thruster allocation as follows:

$$\boldsymbol{\tau}_c = \boldsymbol{T}(\boldsymbol{u} + \boldsymbol{d}), \tag{7}$$

### 2.4 Plant model

Under the considered hypotheses above the considered dynamic positioning (DP) model has the following form:

$$\begin{aligned} \dot{\boldsymbol{\xi}} &= \boldsymbol{A}_w\boldsymbol{\xi} + \boldsymbol{E}_w\boldsymbol{w}_w, \\ \dot{\boldsymbol{\eta}}_{LF} &= \boldsymbol{R}(\psi)\boldsymbol{\nu}_{LF}, \\ \dot{\boldsymbol{b}} &= \boldsymbol{w}_b, \\ \dot{\boldsymbol{d}} &= \boldsymbol{w}_d, \\ \boldsymbol{M}\dot{\boldsymbol{\nu}}_{LF} &= -\boldsymbol{D}\boldsymbol{\nu}_{LF} + \boldsymbol{T}(\boldsymbol{u}+\boldsymbol{d}) - \boldsymbol{R}(\psi)^T\boldsymbol{b} + \boldsymbol{w}_{\nu_{LF}}, \\ \boldsymbol{\eta}_m &= \boldsymbol{\eta}_{LF} + \boldsymbol{\eta}_{WF} + \boldsymbol{w}_\eta. \end{aligned} \tag{8}$$

where $\boldsymbol{w}_{\nu_{LF}} \sim \mathcal{N}(\boldsymbol{0}, \boldsymbol{Q}_\nu)$ is a white noise process representing the model inaccuracies. Defining the state vector $\boldsymbol{x} = [\boldsymbol{\xi}^T, \boldsymbol{\eta}_{LF}^T, \boldsymbol{b}^T, \boldsymbol{d}^T, \boldsymbol{\nu}_{LF}^T]^T \in \Re^{21}$ and the measured ship position $\boldsymbol{\eta}_m \in \Re^3$ in the $\{n\}$ frame as the superposition of LF and WF dynamics, the DP model in (8) has the following non linear state space form:

$$\dot{\boldsymbol{x}} = \underbrace{\begin{bmatrix} \boldsymbol{A}_w & 0 & 0 & 0 & 0 \\ 0 & 0 & 0 & 0 & \boldsymbol{R}(\psi) \\ 0 & 0 & 0 & 0 & 0 \\ 0 & 0 & 0 & 0 & 0 \\ 0 & 0 & -\boldsymbol{M}^{-1}\boldsymbol{R}(\psi)^T & \boldsymbol{M}^{-1}\boldsymbol{T} & -\boldsymbol{M}^{-1}\boldsymbol{D} \end{bmatrix}}_{\boldsymbol{f}(x)} \boldsymbol{x} + \underbrace{\begin{bmatrix} 0 \\ 0 \\ 0 \\ 0 \\ \boldsymbol{M}^{-1}\boldsymbol{T} \end{bmatrix}}_{\boldsymbol{B}} (\boldsymbol{u}+\boldsymbol{d}) + \underbrace{\begin{bmatrix} \boldsymbol{E}_w & 0 & 0 & 0 \\ 0 & 0 & 0 & 0 \\ 0 & \boldsymbol{I} & 0 & 0 \\ 0 & 0 & \boldsymbol{I} & 0 \\ 0 & 0 & 0 & \boldsymbol{M}^{-1} \end{bmatrix}}_{\boldsymbol{E}} \boldsymbol{w}, \quad \boldsymbol{\eta}_m = \underbrace{\begin{bmatrix} \boldsymbol{C}_w & \boldsymbol{I} & 0 & 0 & 0 \end{bmatrix}}_{\boldsymbol{H}} \boldsymbol{x} + \boldsymbol{w}_{\boldsymbol{\eta}}, \tag{9}$$

where $\boldsymbol{w} = [\boldsymbol{w}_w^T, \boldsymbol{w}_b^T, \boldsymbol{w}_d^T, \boldsymbol{w}_\nu^T]^T$ is the state white noise vector with covariance $\boldsymbol{Q} = \text{diag}\{\boldsymbol{Q}_w, \boldsymbol{Q}_b, \boldsymbol{Q}_d, \boldsymbol{Q}_\nu\}$, $\boldsymbol{f}(\boldsymbol{x})$ is the non linear state transition term, $\boldsymbol{B}$ is the control input matrix and $\boldsymbol{E}$ is the state disturbance matrix, $\boldsymbol{H}$ is the output transition matrix and $\boldsymbol{w}_\eta \sim \mathcal{N}(\boldsymbol{0}, \boldsymbol{Q}_\eta)$ is the white noise process modeling the measurement error.

## 3. WAVE FILTERING

In order to avoid large chattering phenomena in the control system due to uncontrollable oscillatory motion, produced by the 1-st order waves, the LF and WF contribution to the ship motion must be separated. For this purpose a wave filter estimates the low-frequency and the wave frequency motion $\boldsymbol{\eta}_{LF}$ and $\boldsymbol{\eta}_{WF}$ respectively. The low frequency GPS measurements justifies (Fossen [2011]) the implementation of the discrete-time Extended Kalman Filtering Benetazzo et al. [2012] to estimate the motion components based on the model (9). Assuming the control input $\boldsymbol{u}(t) = \boldsymbol{u}(k)$ for $t \in [kT_s, (k+1)T_s]$, where $T_s$ is the sampling time, the models (9) are linearized about the current state prediction estimate $\hat{\boldsymbol{x}}_{k+1/k}$ to obtain an extended Kalman filter with an effective state prediction equation. The terms $\boldsymbol{B}$, $\boldsymbol{E}$ and $\boldsymbol{H}$ are linear, the state matrix $\boldsymbol{f}(x)$ is linearized as:

$$\boldsymbol{A}_c = \frac{\partial}{\partial \boldsymbol{x}}\boldsymbol{f}(\boldsymbol{x}) \mid_{\hat{\boldsymbol{x}}_{k+1/k}} \tag{10}$$

The discretization of this linear model, using a Zero Order Hold (ZOH) with period $T_s$, produces the linear discrete-time model of the following form Fossen [2011]:

$$\begin{aligned} &\boldsymbol{x}(k) = \boldsymbol{A}_D(\boldsymbol{x}(k-1)) + \boldsymbol{B}_D\boldsymbol{u}(k-1) + \boldsymbol{E}_D\boldsymbol{w}(k-1) \\ &\boldsymbol{y}(k) = \boldsymbol{H}\boldsymbol{x}(k) + \boldsymbol{w}_\eta(k) \\ &\quad \text{with} \\ &\boldsymbol{A}_D = e^{\boldsymbol{A}_c T_s} \\ &\boldsymbol{B}_D = \left(\int_0^{T_s} e^{\boldsymbol{A}_c\tau} d\tau\right)\boldsymbol{B} = \boldsymbol{A}_c^{-1}(\boldsymbol{A}_D - \boldsymbol{I})\boldsymbol{B} \\ &\boldsymbol{E}_D = \left(\int_0^{T_s} e^{\boldsymbol{A}_c\tau} d\tau\right)\boldsymbol{E} = \boldsymbol{A}_c^{-1}(\boldsymbol{A}_D - \boldsymbol{I})\boldsymbol{E} \\ &\boldsymbol{Q}_D = \int_0^{T_s} e^{\boldsymbol{A}_c\tau}\boldsymbol{Q}e^{\boldsymbol{A}_c^T\tau} d\tau = \boldsymbol{Q}T_s + \left(\boldsymbol{A}_c\boldsymbol{Q} + \boldsymbol{Q}\boldsymbol{A}_c^T\right)\frac{T_s^2}{2} + \boldsymbol{A}\boldsymbol{Q}\boldsymbol{A}^T\frac{T_s^3}{3} \end{aligned} \tag{11}$$

Then the discrete time EKF has the form given in Jetto et al. [1999] and Benetazzo et al. [2012].The implementation of the Kalman filter requires the estimation of the parameter of the model (11). For more details see Fossen [2011] and Fu et al. [2010]. The ship motion $\boldsymbol{\eta}_m$ in Eq. (8) is measured by devices (GPS and compass). These sensors do not work at the same frequency and not all measures are available at each sampling instant. The multi-rate model based on the *delta-functions* is considered. For information about the implementation of the Multirate Kalamn Filter see Benetazzo et al. [2012] and Mora and Tornero [2008].

## 4. DISCRETE TIME VARIABLE STRUCTURE CONTROL

The DP control system, proposed by this paper, is based on the Variable Structure Control, that is a discontinuous nonlinear control, where the control law switches between two functions. The variable structure control law alters the dynamics of the nonlinear system by means of a discontinuous control signal that forces the trajectory of the system state to slide along region with a different control structure. The motion of the system as it slides along these boundaries is called a sliding mode and the geometrical locus $\boldsymbol{s}$ consisting of the boundaries is called the sliding surface. Control design requires to select the sliding surface such that the system trajectory exhibits stable dynamics behavior when confined to it and find a feedback control law such that the system trajectory intersects and stays close to the sliding surface. The aim is to force the ship position to follow a behaviour defined by sliding motion surfaces, which dynamics must be asymptotically stable, Utkin [1992]. The Discrete-Time version of the Variable Structure Control (DTVSC), Furuta [1990], Corradini et al. [2012] allows the implementation of the control law on the DP computer system, while ensuring robustness with respect to model uncertainties and input disturbances acting on the actuators. Moreover in this paper the DTVSC is proposed for handling the thruster failures above described.

### *4.1 Control Model*

The DTVSC proposed in this paper consider the control of ship position $\boldsymbol{\eta}$ by using the velocities $\boldsymbol{\nu}_{LF}$ in the $\{b\}$ frame. The control model is derived from (8) and takes the following form:

$$\dot{\boldsymbol{\nu}}_{LF} = -\boldsymbol{M}^{-1}\boldsymbol{D}\boldsymbol{\nu}_{LF} - \boldsymbol{M}^{-1}\boldsymbol{R}(\psi)\boldsymbol{b} + \boldsymbol{M}^{-1}\boldsymbol{T}\boldsymbol{u} + \boldsymbol{M}^{-1}\boldsymbol{T}\boldsymbol{d}. \tag{12}$$

The DTVSC is applied to the discretization of the ship dynamics model (12) with the sampling time $T_s$ using a Zero Order Hold (ZOH):

$$\boldsymbol{\nu}_{LF}(k+1) = \underbrace{\mathrm{e}^{-\boldsymbol{M}^{-1}\boldsymbol{D}T_s}}_{\boldsymbol{F}}\boldsymbol{\nu}_{LF}(k) + \underbrace{\int_0^{T_s} \mathrm{e}^{-\boldsymbol{M}^{-1}\boldsymbol{D}\sigma}\boldsymbol{M}^{-1}\,\mathrm{d}\sigma\,\boldsymbol{u}(k)}_{\boldsymbol{G}} + \underbrace{-\int_0^{T_s} \mathrm{e}^{-\boldsymbol{M}^{-1}\boldsymbol{D}\sigma}\boldsymbol{M}^{-1}\boldsymbol{R}(\psi(\sigma))\boldsymbol{b}(\sigma)\,\mathrm{d}\sigma}_{\boldsymbol{G}_b} + \underbrace{\int_0^{T_s} \mathrm{e}^{-\boldsymbol{M}^{-1}\boldsymbol{D}\sigma}\boldsymbol{M}^{-1}\boldsymbol{T}\boldsymbol{d}(\sigma)\,\mathrm{d}\sigma}_{\boldsymbol{G}_d} \tag{13}$$

Denoting the control generalized force vector in body-fixed $\{b\}$ frame as:

$$\boldsymbol{\tau}^*(k) = [\tau_u^*(k)\tau_v^*(k)\tau_r^*(k)]^T = \boldsymbol{G}\boldsymbol{u}(k) \tag{14}$$

the discrete time model used for deriving the control law takes the form:

$$\boldsymbol{\nu}_{LF}(k+1) = \boldsymbol{F}\boldsymbol{\nu}_{LF}(k) + \boldsymbol{\tau}^*(k) + \boldsymbol{G}_b(k) + \boldsymbol{G}_d(k) \tag{15}$$

### *4.2 Robustness specifications*

The maximum value of allowable environmental and input disturbance as well as uncertainties of the model parameters the control system can handle characterizes the robustness of the proposed approach.

To account for possible model uncertainties, it is assumed that model parameters may differ from their nominal values $\bar{\boldsymbol{F}}$ for some known bounded quantities $\boldsymbol{\Delta F}$:

$$\boldsymbol{F} = \bar{\boldsymbol{F}} + \boldsymbol{\Delta F}; \tag{16}$$

It is assumed disturbances are bounded by the known bounds:

$$\boldsymbol{G}_b(k) < \boldsymbol{\Delta G_b}, \quad \boldsymbol{G}_d(k) < \boldsymbol{\Delta G_d}. \tag{17}$$

### *4.3 Problem Definition*

A dynamic positioning (DP) control system maintains floating structures in fixed position or pre-determined track for marine operation purposes exclusively by means of active thrusters, Sorensen [2011].Therefore, the Dynamic Positioning control problem of a marine surface vessel can be formulated as:

***O*:** the objective is to maintain the ship in a reference position $\boldsymbol{\eta}^*$ in the $\{n\}$ frame or to mantain a reference track $\boldsymbol{\eta}^*(k)$;

***SP*:** the set of specifications for the reference track;

***CL*:** the control law belongs to the class of closed loop discrete time variable structure control systems.

For the DP system the dynamic positioning error between the reference position and orientation and the measured position and orientation has the form:

$$\boldsymbol{\Delta\eta} = \boldsymbol{\eta}^* - \boldsymbol{\eta}_m. \tag{18}$$

In order to solve the DP problem the dynamic positioning error defined in the $\{n\}$ is conveniently reformulated in the $\{b\}$ frame in terms of velocity tracking error. The velocity tracking error is defined as the difference between the ship low frequency velocity $\boldsymbol{\nu}_{LF}(k) = [u_{LF}(k), v_{LF}(k), r_{LF}(k)]^T$ and the reference velocity $\boldsymbol{\nu}^*_{LF}(k) = [u^*(k), v(k)^*, r^*(k)]^T$, obtained using the inverse kinematic equation of (2) and the imposed reference track (18) in the $\{n\}$ frame and it has the following form:

$$\boldsymbol{\Delta\nu}_{LF}(k) = \boldsymbol{\nu}_{LF}(k) - \boldsymbol{\nu}^*_{LF}(k) \tag{19}$$

The following bounds for the reference velocity and acceleration are considered:

- The reference acceleration in the $\{b\}$ frame is bounded by the maximum generalized acceleration $\boldsymbol{\varrho}^* = [\varrho_u^*\,\varrho_v^*\,\varrho_r^*]^T$ during DP operation:

$$\begin{array}{l} |u^*_{LF}(k+1) - u^*_{LF}(k)| < \varrho_u^* \\ |v^*_{LF}(k+1) - v^*_{LF}(k)| < \varrho_v^* \\ |r^*_{LF}(k+1) - r^*_{LF}(k)| < \varrho_r^* \end{array} \qquad \forall k. \tag{20}$$

- The reference velocity in the $\{b\}$ frame is bounded by the maximum generalized speed $\boldsymbol{\mathcal{V}} = [\mathcal{V}_u\,\mathcal{V}_v\,\mathcal{V}_r]^T$ during DP operation:

$$\begin{array}{l} |u_{LF}(k)| < \mathcal{V}_u \\ |v_{LF}(k)| < \mathcal{V}_v \\ |r_{LF}(k)| < \mathcal{V}_r \end{array} \qquad \forall k. \tag{21}$$

### *4.4 Control Design Procedure*

The Discrete-Time Variable Structure Control is proposed to solve the DP problem defined in Section 4.3, with the robustness specifications in Section 4.2. A sliding mode where the system trajectory exhibits stable dynamics behavior is called quasi-sliding motion on the surface $\boldsymbol{s}(k) = 0$. As stated in Furuta [1990] and Sarpturk et al. [1987], that is achieved if and only if the following Discrete-Time Sliding Mode Existence Condition (DSMEC) is verified by the sliding dynamics:

$$\begin{array}{l} |s_u(k+1)| < |s_u(k)| \\ |s_v(k+1)| < |s_v(k)| \\ |s_r(k+1)| < |s_r(k)| \end{array} \qquad \forall k. \tag{22}$$

In order to design the variable structure controller the following two-steps design procedure is proposed (Furuta [1990], Sarpturk et al. [1987]):

(1) selection of the sliding surface $\boldsymbol{s}(k)$ with stable internal dynamics;
(2) computation of a control law which steers the closed-loop system towards the sliding surface and ensures the system trajectories to stay as close as possible to the surface;

*Sliding surface selection* To solve the DP tracking problem by the above recolled design procedure the tracking error in (19) is minimized using the following two-step sliding surface:

$$\underbrace{\begin{bmatrix} s_u(k) \\ s_v(k) \\ s_r(k) \end{bmatrix}}_{\boldsymbol{s}(k)} = \boldsymbol{\Delta\nu}_{LF}(k) + \boldsymbol{\Lambda}_1 \boldsymbol{\Delta\nu}_{LF}(k-1) + \boldsymbol{\Lambda}_2 \boldsymbol{\Delta\nu}_{LF}(k-2) = 0 \quad (23)$$

Stable internal dynamics of this sliding surface is ensured choice of the parameters $\boldsymbol{\Lambda}_1 = \mathrm{diag}\,(\lambda_{1,u}, \lambda_{1,v}, \lambda_{1,r}), \boldsymbol{\Lambda}_2 = \mathrm{diag}\,(\lambda_{2,u}, \lambda_{2,v}, \lambda_{2,r})$ according to the following condition:

$$\{\{\lambda_{1,i}, \lambda_{2,i}\}/ \left|\mathrm{Roots}\left(p(\delta) = \delta^2 + \lambda_{1,i}\delta + \lambda_{2,i}\right)\right| < 1\} \quad \forall i \in \{u, v, r\} \quad (24)$$

*Computation of the control law* Given the DP discrete time model (15) and two-steps sliding surfaces (23) satisfying (24), the following Discrete-Time Variable Structure Control Law:

$$\boldsymbol{\tau}^*(k) = \boldsymbol{\tau}^*_{eq}(k) + \boldsymbol{\tau}^*_n(k) \quad (25)$$

satisfies the Discrete-Time Sliding Mode Existence Condition (22), where the equivalent control term $\boldsymbol{\tau}_{eq}$ is given by:

$$\boldsymbol{\tau}^*_{eq}(k) = \boldsymbol{\nu}_{LF}(k) - \bar{\boldsymbol{F}}\boldsymbol{\nu}_{LF}(k) - \boldsymbol{\Lambda}_1 \boldsymbol{\Delta\nu}_{LF}(k) - \boldsymbol{\Lambda}_2 \boldsymbol{\Delta\nu}_{LF}(k-1) \quad (26)$$

and the discontinuous control term $\boldsymbol{\tau}_n = \left[\tau^*_{n_u}\ \tau^*_{n_v}\ \tau^*_{n_r}\right]^T$ is given by

$$\tau^*_{n_i}(k) = \begin{cases} \vartheta_i\left(|s_i(k)| - \varrho_i\right) & \text{if } |s_i(k)| > \varrho_i \\ -s_i(k) + \tau^*_{n_i}(k-1) & \text{if } |s_i(k)| \le \varrho_i \end{cases} \quad i \in \{u, v, r\} \quad (27)$$

with parameters $|\vartheta_i| < 1$ with $i \in \{u, v, r\}$ and $\boldsymbol{\varrho} = [\varrho_u\ \varrho_v\ \varrho_r]^T$ given by:

$$\boldsymbol{\varrho} = \boldsymbol{\Delta F \mathcal{V}} + \boldsymbol{\Delta G_b} + \boldsymbol{\Delta G_d} + \boldsymbol{\varrho}^* \quad (28)$$

Moreover, integral action for drift forces compensation is used to minimize the steady state position error $\boldsymbol{\Delta\eta}$, as stated in Loria et al. [2000].

$$\boldsymbol{\tau}_I(k) = \boldsymbol{\tau}_I(k-1) + K_I T_s(\boldsymbol{\eta}^*_{LF}(k-1) - \boldsymbol{\eta}_{LF}(k-1)) \quad (29)$$

In order to obtain zero steady-state errors, it is possible to sum the integral action (29) to DTVSC in the control law, see Fossen [2011]. The final control law is given combining the DTVSC and Integral actions:

$$\boldsymbol{\tau}_c(k) = \boldsymbol{\tau}^*(k) + \boldsymbol{\tau}_I(k) \quad (30)$$

## 5. EXPERIMENTAL RESULTS

The 1:30 scale model of a naval surveillance vessel operating in the North Sea,the *CyberShip 3* (CS3), was used for testing. This ship is located in a 40m x 6.45m x 1.5m towing tank of the *Marine Cybernetics Laboratory* (MCLab), at the Norwegian University of Science and Technology. The ship is equipped with two azimuth thrusters located at the aft and one at the bow, as shown in Fig. 1. Thrusters positions are $L_{y1} = 0.11m$, $L_{y2} = 0.11m$, $L_{x1} = L_{x2} = 0.789m$ and $L_{x3} = 0.636m$. An azimuth thruster is installed in the bow. It has a mass of m = 75 kg, length of L = 2.27 m and breadth of B = 0.4 m. Referring to Fig. 1, the maximum thrust of the main thrusters is 21.9 N and the maximum thrust of the fore thruster is 10 N. Ship devices and motor drives are controlled by an onboard computer which uses a QNX real-time operating system. The control system presented in this paper is developed under Simulink/Opal RT using developed using rapid prototyping techniques and automatic code generation under Matlab/Simulink and Opal on the host PC, built and downloaded to the onboard PC using a wireless Ethernet. Internal variable are sent to the host PC by wireless communication, in a master/slave SW architecture. Tracking a model vessel's motions under different wave, current or wind conditions is one of the fundamental tasks at a hydrodynamics lab or a naval test site. Traditionally, this has been accomplished with potentiometer systems attached to a model or with bulky and expensive gyroscopes and accelerometers. A Global Positioning System provides 6DOF real-time motion of the vessel, thus Earth-fixed position and heading. The MCU consists of onshore 3-cameras mounted on the towing carriage, which puts the model and the markers mounted on the vessel in the line of sight. The cameras emit infrared light and receive the light reflected from the low-mass optical targets. To simulate the different sea conditions a wave maker system, produced by the Danish Hydraulic Institute (DHI), is used. The wave maker is a 6 meter width single paddle and is operated with a electrical servo actuator. The system is equipped with a Active Wave Absorption Control System (AWACS 2). The system has a DHI Wave Synthesizer which can produce regular and irregular waves. JONSWAP spectrum has been used for simulating the different sea conditions for the experiments, stated in Table 1. Results of experiments are compared with Matlab/Simulink simulations, using the same setup and model, with MCSim software.

The performance index is considered for a quantitative comparison between results of various simulations. The performance index used here is the Integral of Squared Error *ISE*. For the DP system index depend on the error between position and orientation simulated and position and orientation measured by sensors, namely

Table 1. Sea Conditions

| Sea State | $H_s$ (m) | $\omega_0$ (rad/s) |
|---|---|---|
| Calm | [0 0.1] | [1.11 1.8] |
| Moderate | [0.1 1.69] | [0.74 1.11] |
| High | [1.69 6] | [0.53 0.74] |

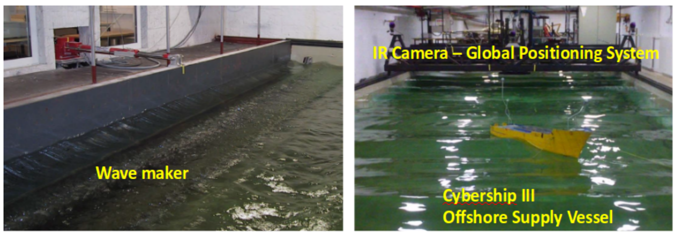


Fig. 2. Experimental Setup in MCLab

Table 3. ISE performance index

| | $n$ (surge position) | | $e$ (sway position) | | $\psi$ (yaw rotation) | |
|---|---|---|---|---|---|---|
| | Sim. | Exp. | Sim. | Exp. | Sim. | Exp. |
| Case 1 | 0.023 | 0.037 | 0.021 | '0.043 | 0.151 | 0.232 |
| Case 2 | 0.073 | 0.113 | 0.047 | 0.079 | 0.364 | 0.418 |
| Case 3 | 0.057 | 0.078 | 0.052 | 0.072 | 0.153 | 0.214 |

Table 2. Reference positions and headings

| Case | Time (s) | n (m) | e (m) | $\psi$ (deg) |
|---|---|---|---|---|
| 1 | 0-1000 | 0 | 0 | 0 |
| 1 | 1000-2000 | 2 | 2 | 20 |
| 2 | 0-1000 | 0 | 0 | 0 |
| 2 | 1000-2000 | 2 | 2 | 20 |
| 3 | 0-800 | 2.5 | 1.5 | arctan $(n/e)$ |
| 3 | 800-1400s | 3 | 1.5 | arctan $(n/e)$ |
| 3 | 1400-2000 | 3 | 3.5 | arctan $(n/e)$ |

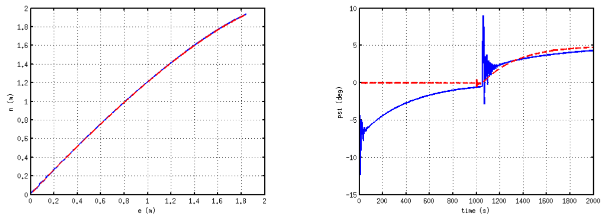

(a) Simulated and experimented path (b) Reference and experimented yaw rotation angle

Fig. 3. CASE 1 - Simulation (red dashed line) and experimental (blue line) position and headings using DTVS controller.

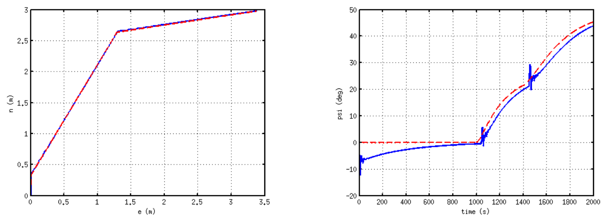

(a) Simulated and experimental path (b) Simulated and experimental yaw rotation angle

Fig. 4. CASE 3 - Simulation (red dashed line) and experimental (blue line) position and headings using DTVS controller.

$\boldsymbol{e(t)} = \boldsymbol{\eta_{des}(t)} - \boldsymbol{\eta(t)}$. The index expression is $ISE = (t_f - t_0)^{-1} \int_{t_0}^{t_f} \boldsymbol{e(t)}^T \boldsymbol{e(t)}\, dt$.

In the following, we show the comparison between the simulated and experimental results, considering the following case scenarios:

**Case 1** The Cybership III holds position in calm sea for 1000 seconds after the waves are full developed and then sails on a short straight movement.

**Case 2** The Cybership III holds position in moderate sea for 1000 seconds after the waves are full developed and then sails on a short straight movement.

**Case 3** The Cybership III sails in moderate sea conditions, with two changes of reference position and headings.

Reference positions in the $\{n\}$ frame are shown in Table 2. Environmental conditions during tests, in terms of significant wave height $H_s$, modal frequency $w_0$ are shown in Table 1. Results in term of ISE performance index are in Table 3. Results from CASE 1 experiments and simulations are shown in Fig. 3. Results from the CASE 3 experiments simulations are shown in Fig. 4.

Experimental results show that the DTVS controller guarantees a satisfactory performance with respect to the simulations controller in every case considered. Results of the CASE 1 simulations, depicted in Fig. 3(b), show that the DTVSC controller rapidly brings the system state nearby the sliding surfaces, while the integral action counteract the 2-nd order slowly varying drift forces. While Case 3 simulation results in Fig. 4(b) show that DTVS control system performs smooth during reference position changes, notably for the yaw rotation angle. Results in Table 3 show that the worse environmental conditions of CASE 2 respect to CASE 1 are reflected by far larger ISE performance indices, but in all the cases the ISE index value is the same order of magnitude both for simulations and experimental tests, corroborating the validity of the approach.

## 6. CONCLUSION

The problem of dynamic positioning plays a key role in all those cases where it is not possible to anchor the ship at the seabed, or where the ship's position is bound to a specific point on the bottom. In this paper an architecture for the dynamic positioning control using sliding mode control and discrete-time models is tested in an experimental setup. Simulations confirm the robustness of the control scheme for calm and moderate seas, corroborating simulation results. ISE performance index value is selected to classify test results, same order of magnitude are found for simulations and experimental tests, corroborating the validity of the approach.

## REFERENCES


Jens G Balchen, Nils A Jenssen, Eldar Mathisen, and Steinar Sæ lid. A Dynamic Positioning System Based on Kalman Filtering and Optimal Control. *Modeling, Identification and Control*, 1(3):135–163, 1980.

Flavia Benetazzo, Gianluca Ippoliti, Sauro Longhi, and Paolo Raspa. Discrete Time Variable Structure Control for the Dynamic Positioning of an Offshore Supply Vessel. In *Preprints of the 2012 IFAC Workshop on Automatic Control in Offshore Oil and Gas Production*, 2012.

M.L. Corradini, G. Ippoliti, S. Longhi, and G. Orlando. A quasi-sliding mode approach for robust control and speed estimation of PM synchronous motors. *IEEE Transactions on Industrial Electronics*, 59(2):1096 – 1104, Feb. 2012.

Thor I. Fossen. *Handbook of Marine Craft Hydrodynamics and Motion Control*. John Wiley and Sons, Ltd, Chichester, UK, April 2011. ISBN 9781119994138.

T.I. Fossen and T. Perez. Kalman filtering for positioning and heading control of ships and offshore rigs. *IEEE Control Systems Magazine*, CST-29(6):32–46, 2009.

Mingyu Fu, Fuguang Ding, Meng Li, and Pengfei Yi. A nonlinear estimate filter designed for ship dynamic positioning. In *8th IEEE International Conference on Control and Automation*, pages 914–919, June 2010.

Katsuhisa Furuta. Sliding mode control of a discrete system. *Systems and Control Letters*, 14(2):145 – 152, 1990. ISSN 0167-6911.

L. Jetto, S. Longhi, and G. Venturini. Development and experimental validation of an adaptive extended kalman filter for the localization of mobile robots. *IEEE Transactions on Robotics and Automation*, 15:219–229, 1999.

A. Loria, T.I. Fossen, and E. Panteley. A separation principle for dynamic positioning of ships: theoretical and experimental results. *Control Systems Technology, IEEE Transactions on*, 8(2):332 –343, mar 2000. ISSN 1063-6536.

M C Mora and J Tornero. Path planning and trajectory generation using multi-rate predictive Artificial Potential Fields. In *IEEE/RSJ International Conference on Intelligent Robots and Systems*, pages 2990–2995, 2008.

D.T. Nguyen and A.J. Sorensen. Setpoint chasing for thruster-assisted position mooring. *Oceanic Engineering, IEEE Journal of*, 34(4):548–558, oct. 2009. ISSN 0364-9059. doi: 10.1109/JOE.2009.2034553.

T Perez, T I Fossen, and A J Sø rensen. A discussion about seakeeping and manoeuvring models for surface vessels. Mss-tr-001, Centre for Ships and Ocean Structures (CESOS), Norwegian University of Science and Technology NTNU, Trondheim, Norway, 2004. URL `http://www.cesos.ntnu.no/mss`.

S.Z. Sarpturk, Y. Istefanopulos, and O. Kaynak. On the stability of discrete-time sliding mode systems. *IEEE Transaction of Automatic Control*, AC-32:930–932, 1987.

Asgeir J. Sorensen. A survey of dynamic positioning control systems. *Annual Reviews in Control*, 35(1):123 – 136, 2011. ISSN 1367-5788.

Eduardo A Tannuri and Adriana C Agostinho. Higher order sliding mode control applied to dynamic positioning systems. In *Proc. of the 8th IFAC Conference on Control Applications in MarineSystems*, pages 132–137, Rostock-Warnemunde, Germany, September 2010.

Vadim Utkin. *Sliding modes in control and optimization*. Springer-Verlag, Berlin Allemagne, 1992. ISBN 9783540535164.

Guoqing Xia, Xiaocheng Shi, Mingyu Fu, Hongjian Wang, and Xinqian Bian. Design of dynamic positioning systems using hybrid CMAC-based PID controller for a ship. In *Mechatronics and Automation, 2005 IEEE International Conference*, volume 2, pages 825 – 830 Vol. 2, 2005. doi: 10.1109/ICMA.2005.1626657.